UC Irvine

Title
Three decades of global methane sources and sinks

Permalink
https://escholarship.org/uc/item/04p4q8dd

Journal
Nature Geoscience, 6(10)

ISSN
1752-0894

Authors
Kirschke, S
Bousquet, P
Ciais, P
et al.

Publication Date
2013-10-01

DOI
10.1038/ngeo1955

Copyright Information

Peer reviewed

Three decades of global methane sources and sinks

Stefanie Kirschke *et al.**

Methane is an important greenhouse gas, responsible for about 20% of the warming induced by long-lived greenhouse gases since pre-industrial times. By reacting with hydroxyl radicals, methane reduces the oxidizing capacity of the atmosphere and generates ozone in the troposphere. Although most sources and sinks of methane have been identified, their relative contributions to atmospheric methane levels are highly uncertain. As such, the factors responsible for the observed stabilization of atmospheric methane levels in the early 2000s, and the renewed rise after 2006, remain unclear. Here, we construct decadal budgets for methane sources and sinks between 1980 and 2010, using a combination of atmospheric measurements and results from chemical transport models, ecosystem models, climate chemistry models and inventories of anthropogenic emissions. The resultant budgets suggest that data-driven approaches and ecosystem models overestimate total natural emissions. We build three contrasting emission scenarios — which differ in fossil fuel and microbial emissions — to explain the decadal variability in atmospheric methane levels detected, here and in previous studies, since 1985. Although uncertainties in emission trends do not allow definitive conclusions to be drawn, we show that the observed stabilization of methane levels between 1999 and 2006 can potentially be explained by decreasing-to-stable fossil fuel emissions, combined with stable-to-increasing microbial emissions. We show that a rise in natural wetland emissions and fossil fuel emissions probably accounts for the renewed increase in global methane levels after 2006, although the relative contribution of these two sources remains uncertain.

Reconstructions of atmospheric methane (CH$_4$) concentrations between 1850 and the 1970s have been made using air trapped in polar ice cores and compacted snow. The data reveal an exponential increase in CH$_4$ levels in the atmosphere from 830 ppb to 1500 ppb in the late 1970s[1]. Direct measurements of CH$_4$ in the atmosphere began in 1978[2], and reached global coverage after 1983. Today, CH$_4$ concentrations can be assessed using discrete air samples collected regularly at the surface, continuous measurements made at the surface[2–6] or in the troposphere[7–9], and remotely sensed measurements of atmospheric CH$_4$ columns retrieved from the surface or from space[10–12] (see Supplementary Section ST1). Surface-based observations from four networks (National Oceanic and Atmospheric Administration, NOAA[13]; Advanced Global Atmospheric Gases Experiment, AGAGE[14]; Commonwealth Scientific and Industrial Research Organization, CSIRO[5]; and University of California Irvine, UCI[15]) show consistent changes in the global growth rate of annual CH$_4$ concentrations since 1980 (Fig. 1 and Supplementary Section ST1). The agreement between these networks has improved with increasing coverage. The standard deviation for the global annual growth rate decreased from ±3.3 ppb yr^{-1} in the 1980s to ±1.3 ppb yr^{-1} in the 2000s. These data reveal a sustained increase in atmospheric CH$_4$ levels in the 1980s (by an average of 12 ± 6 ppb yr^{-1}), a slowdown in growth in the 1990s (6 ± 8 ppb yr^{-1}), and a general stabilisation from 1999 to 2006 to 1773 ± 3 ppb. Since 2007, CH$_4$ levels have been rising again[14], and reached 1799 ± 2 ppb in 2010. This increase reflects a recent imbalance between CH$_4$ sources and sinks that is not yet fully understood[13].

Previous reviews of the global CH$_4$ budget have focused on results from a few studies only[13,16–19]. These studies covered different time windows and employed different assumptions, making it difficult to interpret the decadal changes presented. Only very few studies addressed multi-decadal changes in CH$_4$ levels[20,21]. Here we construct a global CH$_4$ budget for the past three decades by combining bottom-up and top-down estimates of CH$_4$ sources and the chemical CH$_4$ sink (Box 1). We use chemical transport models — constrained by atmospheric CH$_4$ measurements — to estimate CH$_4$ fluxes using top-down atmospheric inversions. We compare these fluxes with those simulated by ecosystem models of wetland and biomass burning emissions and by data-driven approaches for other natural sources (Methods and Supplementary Section II). We also gather recent data from fossil fuel CH$_4$ emission inventories based on energy use statistics, and from agricultural and waste inventories based on livestock and rice paddy statistical data.

Sources and sinks

The global atmospheric CH$_4$ budget is determined by many terrestrial and aquatic surface sources, balanced primarily by one sink in the atmosphere. CH$_4$ emissions can be broadly grouped into three categories: biogenic, thermogenic and pyrogenic. Biogenic sources contain CH$_4$-generating microbes (methanogens)[17], and comprise anaerobic environments such as natural wetlands and rice paddies, oxygen-poor freshwater reservoirs (such as dams), digestive systems of ruminants and termites, and organic waste deposits (such as manure, sewage and landfills). Thermogenic CH$_4$, formed over millions of years through geological processes, is a fossil fuel. It is vented from the subsurface into the atmosphere through natural features (such as terrestrial seeps, marine seeps and mud volcanoes), and through the exploitation of fossil fuels, that is, through the exploitation of coal, oil and natural gas. Pyrogenic CH$_4$ is produced by the incomplete combustion of biomass and soil carbon during wildfires, and of biofuels and fossil fuels. These three types of emissions have different isotopic δ^{13}C signatures (δ^{13}C = [(^{13}C/^{12}C)$_{sample}$/(^{13}C/^{12}C)$_{standard}$] − 1) × 1000): −55 to −70‰ for biogenic emissions, −25 to −55‰ for thermogenic emissions, and −13 to −25‰ for pyrogenic emissions[20,22,23]. The isotopic composition of atmospheric CH$_4$ — measured at a subset of surface stations — has therefore been used to constrain its source[20–24]. CH$_4$ emissions by living plants under aerobic conditions do not seem to play a significant role in the global CH$_4$ budget (Supplementary Section ST8); some very large[25] estimates of this source published in 2006 have not been confirmed[26].

The primary sink for atmospheric CH$_4$ is oxidation by hydroxyl radicals (OH), mostly in the troposphere, which accounts for around 90% of the global CH$_4$ sink. Additional oxidation sinks include methanotrophic bacteria in aerated soils[27,28] (~4%), reactions with
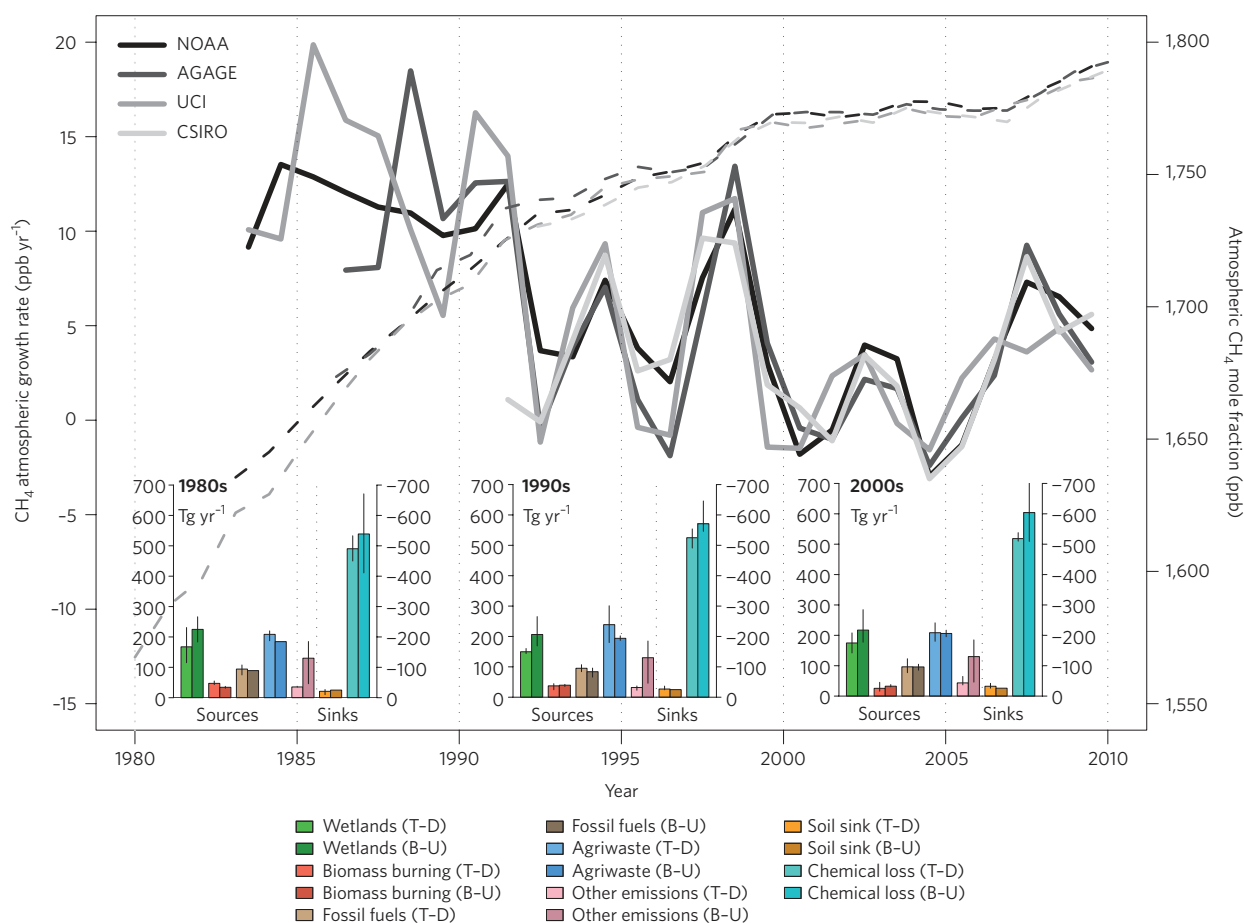
813

Figure 1 | Evolution of the atmospheric global mole fraction, growth rate and budget of methane for the past three decades. The mole fraction (dashed lines) and growth rate (solid lines) from NOAA, AGAGE, UCI and CSIRO networks are shown in varying shades of black/grey. Bar charts show global decadal surface emissions and sinks calculated from top-down (T–D, light-coloured bars) and bottom-up (B–U, dark-coloured bars) approaches. Categories are split into: natural wetlands, biomass burning, fossil fuels, agriculture and waste, other sources (see Table 1), soil uptake and chemical loss by OH oxidation. Error bars spread between minimum and maximum values.

chlorine radicals and atomic oxygen radicals in the stratosphere[17] (~3%), and reactions with chlorine radicals from sea salt in the marine boundary layer[29] (~3%).

Global decadal budget

We combine state-of-the-art top-down and bottom-up approaches (Box 1) using a consistent methodology (see Methods) to assess global CH_4 sources and sinks over the past three decades. At the global scale for the 2000s, top-down inversions yield total global emissions of 548 Tg of CH_4 per year with a minimum–maximum range of 526–569 (six models in Table 1) and a global sink of 540 [514–560] Tg CH_4 yr^{-1}. The source–sink mismatch reflects the observed average imbalance of 6 Tg CH_4 yr^{-1} of the CH_4 growth rate in the 2000s, which is smaller than that of the 1980s and 1990s (34 Tg CH_4 yr^{-1} and 17 Tg CH_4 yr^{-1}, respectively; Fig. 1). In fact, stabilization of atmospheric CH_4 prevailed in the early 2000s, and the atmospheric increase resumed after 2006.

Summing up all bottom-up emission estimates, a different picture emerges for the global source for the 2000s. We obtain a value of 678 Tg CH_4 yr^{-1}, which is 20% larger than the inversion-based estimate ($P<0.01$; Table 1). The higher global source in bottom-up estimates is explained by a larger sum of natural emissions (from wetlands, freshwater, and geological sources) than in the inversions (Table 1). For the 2000s, the bottom-up estimate of the total sink is 632 Tg CH_4 yr^{-1}, with a large range (592–785). Most of this sink — 604 Tg CH_4 yr^{-1} — is due to the hydroxyl radical CH_4 sink, as estimated

by the nine bottom-up chemistry climate models (CCMs)[30]. The OH sink simulated by the seven models that run time slices from the 1980s to the 2000s is found to increase with time, which contrasts with the stability of the OH sink inferred from top-down inversions for the 1990s and the 2000s (Table 1). The positive trend in the OH sink in the CCMs can be explained by the fact that the chemical consumption of OH, for instance through reactions with CH_4 and carbon monoxide, is offset by the production of OH through photochemical reactions, involving water vapour, nitrogen oxides and stratospheric ozone. The stable OH sink inferred from top-down inversions relates to the observed atmospheric record of methyl chloroform, which is used to infer OH changes on decadal scales[30].

We group decadal estimates of emissions (top-down and bottom-up) into five categories: natural wetlands; other natural emissions (termites, geological, fresh water systems, permafrost and hydrates); agriculture and waste; fossil fuels; and biomass and biofuel burning (Table 1). Freshwater systems include lakes, reservoirs, streams and rivers. In the 2000s, natural wetland emissions (top-down, 142–208 Tg CH_4 yr^{-1}; and bottom-up, 177–284 Tg CH_4 yr^{-1}) and agriculture and waste emissions (top-down, 180–241 Tg CH_4 yr^{-1}; and bottom-up, 187–224 Tg CH_4 yr^{-1}) dominate CH_4 emissions, followed by anthropogenic fossil fuel emissions, other natural emissions and emissions from biomass and biofuel burning (Table 1). Together with natural CH_4 emissions from lake and freshwater sources[31,32], we find an imbalance of almost 50 Tg CH_4 yr^{-1} (in the 2000s) between the mean global emission and the mean global sink in the

bottom-up approach, which is larger than the observed growth rate of around 6 Tg CH_4 yr^{-1}.

This discrepancy, combined with the fact that the global mean emission is 130 Tg CH_4 yr^{-1} greater in the bottom-up approach than in the top-down approach (Table 1), suggests that CH_4 emissions are overestimated in the bottom-up approach. Indeed, the bottom-up global emission estimate is obtained by adding up independently estimated flux components, and thus lacks a constraint on its global magnitude. In contrast, the global CH_4 emission derived from the top-down approach is constrained at the global scale by the atmospheric CH_4 growth rate, using atmospheric CH_4 measurements, and by the magnitude of the chemical sink, using proxy atmospheric observations, such as the concentration of methyl chloroform, to estimate OH concentrations. Such proxy methods have proven to be reliable indicators of mean OH levels in the troposphere, although their ability to capture OH changes has been widely discussed[33,34]. These proxy methods suggest that the mean global chemical sink for CH_4 derived from bottom-up estimates may also be overestimated, especially in the 2000s (Table 1).

When summing up anthropogenic fossil emissions, natural fossil CH_4 from onshore and offshore seeps[35,36] (part of geological emissions in Table 1) and hydrates, bottom-up total fossil emissions account for 28% (~156 Tg CH_4 yr^{-1}) of the global CH_4 source between 1985 and 2000. This is consistent with an analysis of ^{14}C-CH_4 atmospheric measurements[37] in both hemispheres inferring a 30 ± 2% fossil fraction in the global CH_4 source. However, fossil emissions of this magnitude are not confirmed by a recent analysis of the global atmospheric record of ethane[15], which is co-emitted with geological CH_4. Top-down inversions cannot provide useful information to settle this debate, as they generally do not separate this source from other natural emissions (Table 1). Consideration of the natural fossil CH_4 source, neglected in previous Intergovernmental Panel on Climate Change (IPCC) assessments, thus represents a significant update to the global CH_4 budget, although it is still debated.

Global budget uncertainty

Uncertainties associated with decadal CH_4 budgets are expressed by the minimum–maximum range between different decadal estimates, due to the small number of studies available for calculating reliable standard deviations (Table 1). For the 2000s, the uncertainty range for bottom-up estimates — defined as (max−min)/mean — is 50% for natural wetlands and typically 100% for other natural sources, though the other individual natural sources have smaller fluxes than wetlands. Anthropogenic sources seem to be known more precisely, with an uncertainty range of 30% for agriculture/waste- and fossil-fuel-related emissions, and 20% for biomass burning. The uncertainty range of the global sink is 40%, but drops to 20% when removing one outlier with very high total OH loss in a recent comparison of climate chemistry models[30,38]. Note that the uncertainties reported in Table 1 are correlated to some extent. Because of more recent and robust estimates for each decade, each term in the budget has a smaller error range than in the IPCC AR4 report: 50% smaller for wetlands, 60% smaller for biomass burning, and 40% smaller for agriculture and waste emissions (Table 1).

Natural wetlands have the largest absolute uncertainty of any of the emission categories, with a min–max range of 107 Tg CH_4 yr^{-1} in the bottom-up approach (177–284 Tg CH_4 yr^{-1}). This large range is confirmed by a recent multi-model analysis[39] showing a ±40% range of wetland emissions around an average of 190 Tg CH_4 yr^{-1}. In the three wetland emission models used here[40–42], emissions were calculated for each grid point as the product of a flux rate and a wetland area, both having uncertainties. Uncertainties in wetland extent seem to be the dominant source of discrepancy in modelled CH_4 emissions[39,43].

The OH sink seems to have a smaller error range using proxy methods in the top-down approach (max–min range of 30 Tg CH_4) than in bottom-up CCMs (max–min range of 250 Tg CH_4, dropping to 110 Tg CH_4 when removing one outlier model from the Atmospheric Chemistry and Climate Model Intercomparison Project (ACCMIP)[30,38], in which different humidity and temperature fields cause a large spread of the OH sink[38].

Following IPCC AR5 guidelines for the treatment of uncertainties[44], we defined a level of confidence for both top-down estimates and bottom-up estimates, based on robustness (number of published studies) and agreement (difference between maximum and minimum estimates, relative to the mean). Many studies have focused on constraining the CH_4 budget during the 1990s and 2000s, but fewer estimates are available for the 1980s. As a result,

---

Box 1 | New data to assess the CH_4 budget

The top-down approach is based on atmospheric inversion models, which determine 'optimal' surface fluxes[92,93] that best fit atmospheric CH_4 observations given an atmospheric transport model including chemistry, prior estimates of fluxes, and their uncertainties. Global atmospheric inversions provide a time-varying distribution of CH_4 fluxes, albeit with limited insight into the underlying processes when different sources overlap in the same region. This is, for example, often the case for agricultural, waste and fossil emissions in densely populated areas of east Asia, Europe and North America. We collected results from nine inversion systems (Supplementary Table S1).

The bottom-up approach includes process-based models estimating CH_4 emissions, and CCMs estimating the OH sink. Eight bottom-up models for wetland and fire CH_4 emissions are parameterized with empirical knowledge of local processes and driven by global data sets of climate, or satellite-observed burned area, to simulate CH_4 fluxes on spatial and temporal scales relevant for regional and global budgets (Supplementary Section II). Bottom-up emission inventories[56,81,82] based on energy use, agricultural activity, and emission factors from different sectors provide yearly or decadal mean estimates of anthropogenic waste-related, rice, livestock, biofuel, and fossil fuel emissions, usually at

national scales. Three inventories for anthropogenic emissions are used, updated to 2008 (Supplementary Information).

The photochemical sink of CH_4 is large and difficult to quantify, given the very short lifetime of OH (~1 sec) and its control by a myriad of precursor species. Direct measurements of atmospheric OH radicals do not have the required accuracy and coverage to derive global OH concentrations and consequently the magnitude of the CH_4 sink. We estimated CH_4 loss due to OH from the output of nine numerical CCMs[65], which are categorized here as an atmospheric bottom-up approach. The OH concentration as calculated by CCMs can be further adjusted, at a large scale, by inversions based on measurements of tracers with known emissions and whose dominant sink is oxidation by OH, such as methyl chloroform[34,49,85,94] or chloromethanes[33,34].

Combining top-down and bottom-up approaches allows us to investigate the consistency of each term of the CH_4 budget[21]. In this comparison, it should be noted that bottom-up models and inventories are not independent from inversions, because they are usually used in inversions to prescribe a prior spatial, and sometimes temporal, distribution of the emissions and sinks. However, inversions use independent atmospheric observations to partially correct the prior values.

Table 1 | CH₄ budget for the past three decades.

	Tg CH$_4$ yr^{-1}					
	1980–1989		**1990–1999**		**2000–2009**	
	Top-down	**Bottom-up**	**Top-down**	**Bottom-up**	**Top-down**	**Bottom-up**
Natural sources	203 [150–267]	355 [244–466]	182 [167–197]	336 [230–465]	218 [179–273]	347 [238–484]
Natural wetlands	167 [115–231][19,21,76]	225 [183–266][40,41]	150 [144–160][21,74,77]	206 [169–265][40–42]	175 [142–208][46,53,73,75,77,86]	217 [177–284][40–42]
Other sources	36 [35–36][19,21,76]	130 [61–200]	32 [23–37][21,74,77]	130 [61–200]	43 [37–65][46,53,73,75,77]	130 [61–200]
Fresh water (lakes and rivers)		40 [8–73][31,32]		40 [8–73][31,32]		40 [8–73][31,32]
Wild animals		15 [15–15][16]		15 [15–15][16]		15 [15–15][16]
Wildfires		3 [1–3][16,47,55,88,89]		3 [1–5][16,47,55,88,89]		3 [1–5][16,47,55,88,89]
Termites		11 [2–11][16,48,55,91]		11 [2–22][16,37,87,91]		11 [2–22][16,37,87,91]
Geological (incl. oceans)		54 [33–75][35,55,90]		54 [33–75][35,55,90]		54 [33–75][35,55,90]
Hydrates		6 [2–9][16,36,87]		6 [2–9][16,36,87]		6 [2–9][16,36,87]
Permafrost (excl. lakes and wetland)		1 [0–1][55]		1 [0–1][55]		1 [0–1][55]
Anthropogenic sources	348 [305–383]	308 [292–323]	372 [290–453]	313 [281–347]	335 [273–409]	331 [304–368]
Agriculture and waste	208 [187–220][19,21,76]	185 [172–197][56]	239 [180–301][21,74,77]	188 [177–196][55,56,81]	209 [180–241][46,53,73,75,77]	200 [187–224][55,56,81]
Biomass burning (incl. biofuels)	46 [43–55][19,21,76]	34 [31–37][78,80]	38 [26–45][21,74,77]	42 [38–45][78,80]	30 [24–45][47,53,72,73,75,77]	35 [32–39][47,78,80,89]
Fossil fuels	94 [75–108][19,21,76]	89 [89–89][56]	95 [84–107][21,74,77]	84 [66–96][55,56,81]	96 [77–123][46,53,73,75,77]	96 [85–105][55,56,81]
Sinks						
Soils	21 [10–27][19,21,76]	28 [9–47][27,42]	27 [27–27][21]	28 [9–47][27,42,89]	32 [26–42][46,53,73,75,86]	28 [9–47][27,42,89]
Total chemical loss	490 [450–533][19,21,76]	539 [411–671][21,29,38,83]	525 [491–554][21,83]	571 [521–621][21,29,38,83]	518 [510–538][46,53,73,75,77]	604 [483–738][21,29,38,83]
Tropospheric OH		468 [382–567][30,38]		479 [457–501][30,38]		528 [454–617][30,38]
Stratospheric loss		46 [16–67][22,38,83]		67 [51–83][21,38,83]		51 [16–84][21,38,83]
Tropospheric Cl		25 [13–37][29]		25 [13–37][29]		25 [13–37][29]
TOTALS						
Sum of sources	551 [500–592]	663 [536–789]	554 [529–596]	649 [511–812]	548 [526–569]	678 [542–852]
Sum of sinks	511 [460–559]	539 [420–718]	542 [518–579]	596 [530–668]	540 [514–560]	632 [592–785]
Imbalance (sources−sinks)	30 [16–40]		12 [7–17]		8 [−4–19]	
Atmospheric growth rate	34		17		6	

Top-down and bottom-up estimates are listed separately for the different categories in Fig. 1. For top-down inversions, the 1980s decade starts in 1984. Numbers in square brackets represent minimum and maximum values. A balance with the atmospheric annual increase and the sum of the sources has been assumed for inversions not reporting their global sink. Stratospheric loss for bottom-up is the sum of the loss by radicals, a 10 Tg yr⁻¹ loss due to O(¹D) radicals[22] and a 20–35% contribution due to Cl radicals[29]. Ranges of total chemical loss are about half the reported ranges (for example, [509-619] for the 2000s) when removing one outlier.

estimates for all source categories during the 2000s are more robust, especially for inversions (Fig. 2). Agreement among studies is high (difference is less than 33%) for agriculture and waste (top-down and bottom-up), biomass burning and fossil fuels (bottom-up) and OH loss (top-down), whereas agreement is only medium (33–66% difference) for natural wetlands (top-down and bottom-up), fossil fuel emissions (top-down) and OH sink (bottom-up) estimates. Low agreement (> 66% difference) is found for biomass burning (top-down) and other natural sources (bottom-up). Increasing the number of studies does not necessarily lead to enhanced agreement.

This can be seen for the fossil fuel and other sources categories, partly because of poorly constrained models, and partly because the results from a single new study can produce a large increase in the spread of emission estimates when very few studies are available.

No source or sink category reaches the highest level of confidence (highest agreement and highest robustness), emphasizing the large uncertainties that remain in our understanding of CH₄ emissions. Overall, higher confidence in global emissions is found for agriculture and waste (top-down) than for fossil fuels, the OH sink, natural wetlands and other natural sources.
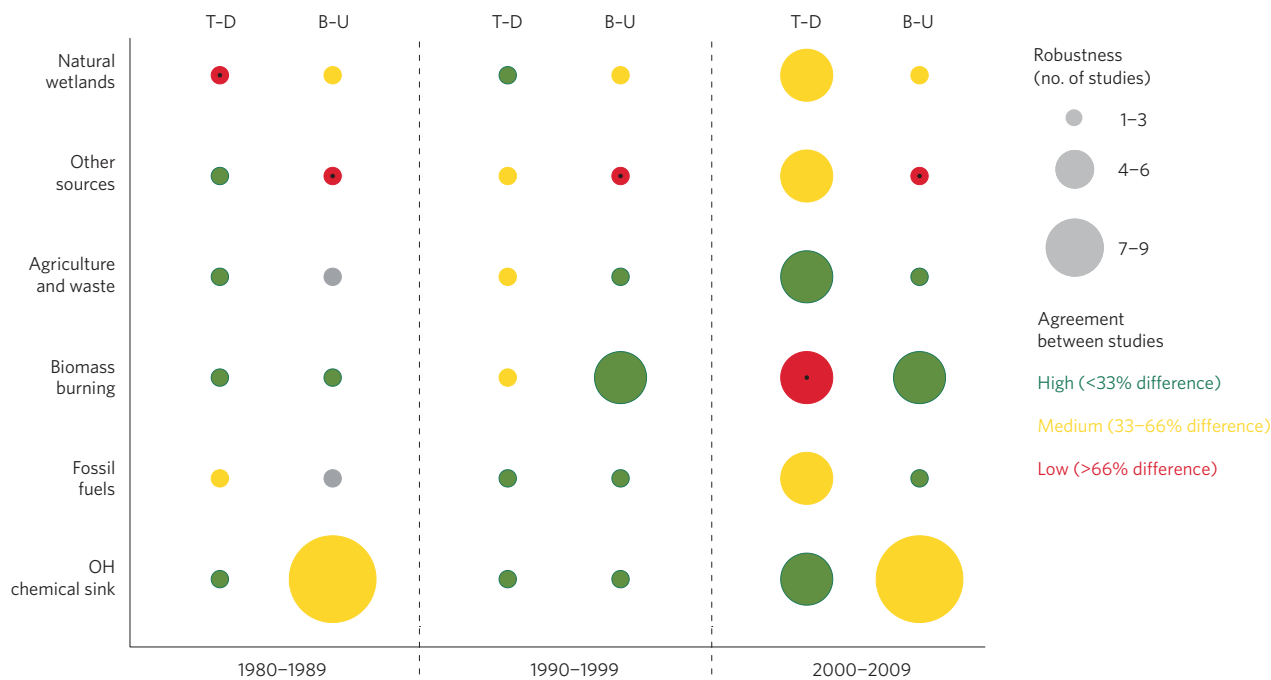
Figure 2 | Evolution of uncertainty on estimates of methane emissions and sinks presented in Table 1. Circle size depicts the robustness of the estimate (number of studies). Circle colour illustrates the level of agreement among studies (min–max ranges): green, high confidence; yellow, medium confidence; red (with black dot), low confidence. Circles are grey when only one study has been used. A large green circle, for example, indicates a very good level of confidence[44].

Regional decadal budget

The geographical breakdown of emissions per category and per region reveals major CH_4 emission zones worldwide and the level of consistency between top-down and bottom-up approaches (Fig. 3 and Supplementary Section ST2 and Tables S2 and S3). Anthropogenic emissions dominate in Europe, North America, China, and the fossil-fuel-producing countries of eastern Europe and central Asia, with good agreement between top-down and bottom-up approaches (Fig. 3). Emission ranges are given in Table S2. Densely populated regions usually emit fossil, agricultural and waste CH_4, making these sources difficult to separate in top-down inversions. Noteworthy is the large range of estimates for anthropogenic fossil CH_4 emissions from China in the top-down approach, possibly due to the low density of atmospheric CH_4 measurements in this region, and to biases in inventories[45]. The large range of anthropogenic CH_4 emission estimates in Europe and North America possibly reflects uncertainties in emission factors, and in the partition between waste and fossil CH_4 sources. In emerging economies, agriculture and waste emissions are highest in China (top-down, 29 Tg CH_4 yr^{-1}; bottom-up, 28 Tg CH_4 yr^{-1}) and India (top-down, 27 Tg CH_4 yr^{-1}; bottom-up, 22 Tg CH_4 yr^{-1}), but are also important in southeast Asia and temperate South America due to extensive rice agriculture and livestock industries (Supplementary Table S2). In India and China, agriculture and waste constitutes the single largest regional source of CH_4. However, per capita CH_4 emissions in India and China are still 35% and 85%, respectively, of the mean for OECD countries.

When aggregated over large regions, wetlands dominate emissions in tropical South America (top-down, 28 Tg CH_4 yr^{-1}; bottom-up, 58 Tg CH_4 yr^{-1}) and Africa (top-down, 36 Tg CH_4 yr^{-1}; bottom-up, 24 Tg CH_4 yr^{-1}), with significant emissions in southeast Asia, temperate South America, boreal North America and boreal Eurasia (Supplementary Table S2). Tropical South America shows the largest regional discrepancy between top-down (17–48 Tg CH_4 yr^{-1}) and bottom-up (39–92 Tg CH_4 yr^{-1}) wetland emissions (Supplementary Tables S2 and S3). The seven inversions

using only surface measurements give the lowest estimates for the 2000s decadal mean wetland emission (17–30 Tg CH_4 yr^{-1}), and the two inversions using SCIAMACHY column satellite data combined with surface measurements[46] (27 and 48 Tg CH_4 yr^{-1}) agree better with bottom-up estimates (39–92 Tg CH_4 yr^{-1}). Only short time series of CH_4 *in situ* measurements are available for inland South America, which makes it one of the least constrained regions for inversions using surface measurements. The wetland models used in this study simulate large emissions in the Amazon region, equatorial tropical Africa, tropical Asia (for example, Bangladesh, India, China and Indonesia), Canada and boreal Eurasia. Simulated emission areas are consistent between models for 66 ± 9% of global wetland emissions over the period 1990–2006 (Supplementary Fig. S0).

When aggregated over large regions, emissions from biomass burning are the largest in Africa (top-down, 9 Tg CH_4 yr^{-1}; bottom-up, 8 Tg CH_4 yr^{-1}) and in tropical South America (top-down, 5 Tg CH_4 yr^{-1}; bottom-up, 4 Tg CH_4 yr^{-1}), but play only a minor role in temperate and boreal regional budgets. The bottom-up estimates are likely to be conservative compared to top-down estimates, as small fires are often undetected by satellite retrieval algorithms[47]. For biomass burning, simulated emission areas are consistent between models for 38 ± 9% of global emissions over the period 1997–2000, revealing robust large emission zones around the thermal equator in Africa (for example, Central African Republic, Democratic Republic of the Congo, Republic of the Congo, Angola, Zambia and Cameroon), central South America (Brazil and Bolivia), Indonesia, and to a lesser extent in eastern Russia, Laos, and Mexico (Supplementary Fig. S0). Emission zones in northern Australia and in boreal regions (Canada and Siberia) can also be clearly identified.

Other natural sources, including termites, lakes and other fresh waters, and onshore geological emissions show maximum values in Africa and tropical South America, due to the relatively strong contribution of emissions by termites[48]. A new empirical model of termite CH_4 emissions developed in this study indicates that Africa and tropical South America are major contributors to the global

termite source, contributing 30% and 36%, respectively, of the total (Supplementary Section ST7). Finally, CH_4 loss due to OH radicals is largest in the tropical atmosphere, both over land and oceans, as the tropics are the major region of OH production[49].

Attribution of temporal changes

Year-to-year variations of CH_4 fluxes have been intensively studied[4,14,21,47,50]. The present study confirms the findings from previous ones showing that, over the last three decades, variations in wetland emissions have dominated the year-to-year variability in surface emissions (Supplementary Fig. S5). Interannual variability in wetland emissions surpasses that of biomass burning emissions, except during intensive fire periods[21,50]. Analyses of anomalies in CH_4 fluxes following the Mount Pinatubo[21,51] eruption in 1991 and the record-high El Niño[47,52] in 1997–1998 are summarized in Supplementary Sections ST4 and ST5. Both models and observations compiled in the present study consistently describe small interannual variability in the OH sink in the 2000s compared with the previous two decades (<3%, 1σ of annual means; Supplementary Section ST6), in line with previously reported estimates (<5%)[34,53].

The observed decadal changes remain much more enigmatic than yearly anomalies (Supplementary Fig. S5). We use a scenario approach, built from our synthesis and from recent publications, to investigate these changes, and the contribution of the different CH_4

sources to them (see Methods). We assume that decadal changes in global mean CH_4 emissions since 1985 are well represented by the mean of those five atmospheric inversions covering the past three decades[53], averaged on a five-year basis (Fig. 4 and Methods). A global mass balance model[54] based on the atmospheric observations of the four surface networks and on possible changes in CH_4 lifetime is used to provide uncertainties on the mean inversion (blue shaded area at the top of Fig. 4). These observation-driven global CH_4 emissions show three distinct regimes: an increase before 1990, an oscillation around a constant mean value during 1990–2005, and an increase after 2006[4,14,53]. A storyline (S_0) is constructed by adding wetland emissions from top-down inversions (average of five inversions) to other estimates (EPA (ref. 55) and EDGARv4.2 (ref. 56) inventories).

1985–2005. The S_0 storyline clearly overestimates global emissions after 1990, which calls for corrections to the magnitude of one or several sources in the S_0 scenario (Fig. 4). Using ethane firn air and atmospheric measurements, two recent studies indicated that CH_4 emissions from the fossil fuel sector decreased between 1985 and 2000 at a rate of −0.4 to −0.8 Tg CH_4 yr^{-1}, and attributed such a decline to decreasing fugitive emissions (leaks during extraction, treatment and use of fossil fuels) from oil and gas industries[15,57]. One of these studies further extended the ethane record up to 2010[15], with either a slower decline or a stabilization of fossil fuel emissions
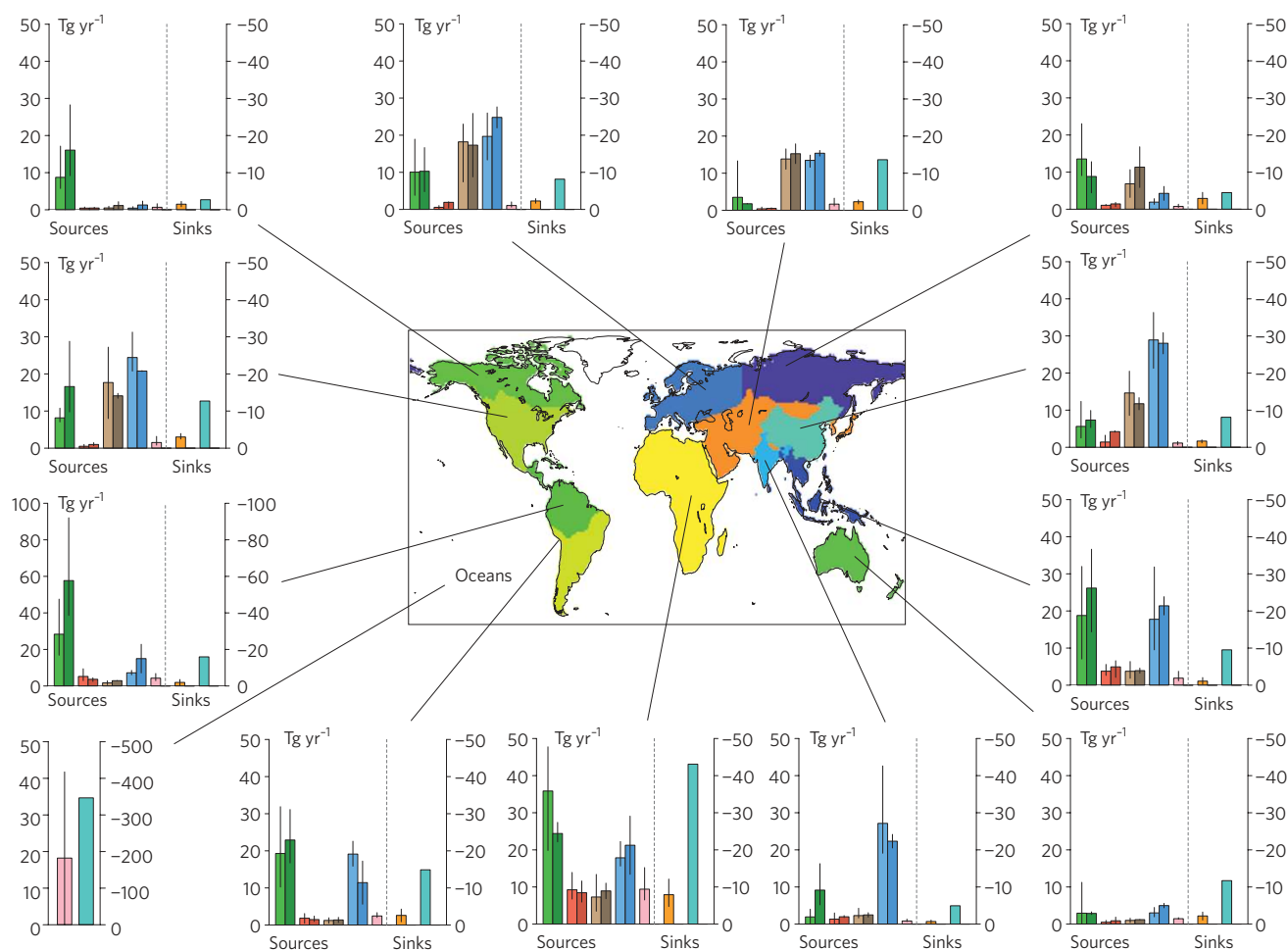

Figure 3 | Regional budgets for 2000–2009 over 13 regions. The considered regions are nine TransCom regions[84], plus separate regions for India, China and southeast Asia, and one region for oceans. Source and sink categories are the same as in Fig. 1. Both top-down (T-D, light-coloured bars) and bottom-up (B-U, dark-coloured bars) approaches are shown. Oceans are considered as one large region (bar chart at the bottom left), with ocean emissions (pink) and chemical loss over the ocean (turquoise). Error bars indicate the spread between the minimum and the maximum values.

after 2000 (see Fig. 4 of ref. 15 and Methods). Indeed, an intensified coal exploitation[45,56] after 2000 may have offset a decline in fugitive emissions. In parallel, rice paddy emissions have decreased (~−0.4 to −0.8 Tg CH_4 yr^{-1}) according to the EDGAR4.2 inventory[56] during the 1980-2000 period, and remained stable between 2000 and 2005. Assuming that CH_4 fossil fuel fugitive emissions decreased between 1985 and 2000[53] and were stable from 2000 to 2005[15], and keeping the other sources as in S_0, leads to a first plausible scenario that is consistent with the observation-driven global emissions (S_1 in Fig. 4). An alternative scenario (S'_1), using bottom-up ecosystem model results for wetland emissions as a storyline instead of top-down inversions, is also consistent with the observation-driven global emissions.

Two different analyses of δ^{13}C-CH_4 isotopic composition trends[58,59] for 1990–2005 reached contradictory conclusions. In one, constant fossil fuel emissions but decreasing microbial emissions in the Northern Hemisphere were inferred[58], the latter mainly attributed to decreasing rice emissions. In the other[59], fossil fuel and microbial emissions remained constant. Assuming constant fossil fuel emissions during 1985–2005 and decreasing microbial emissions[58] produces a second scenario that is mostly consistent with observation-driven global emissions when using wetland fluxes from top-down inversions (S_2 in Fig. 4), but not when using wetland fluxes from bottom-up ecosystem models (S'_2). Assuming decreasing fossil fuel emissions before 1990 (as in S_1), but constant fossil fuel and microbial emissions between 1990 and 2005[59], produces a third scenario that is consistent with observation-driven global emissions, with either top-down or bottom-up wetland emission estimates (S_3 and S'_3 in Fig. 4).

Overall, the three plausible scenarios, among many other possible source compositions matching global decadal changes, suggest that a decrease in fossil fuel CH_4 emissions is a more likely explanation for the stability of global CH_4 emissions between 1990 and 2005 than a reduction in microbial CH_4 emissions. An actual decrease in rice paddy emissions may have been surpassed by an increase in other microbial emissions (natural wetlands, animals, landfills and waste) as found by ecosystem models combined with the EDGAR4.2 inventory. Considering the significant uncertainties reported in a recent isotope study[59] for the 1990–2005 period, decreasing-to-stable fossil fuel emissions, combined with stable-to-increasing total microbial emissions, would reconcile the atmospheric ethane trends with the ^{13}C-CH_4 trends, at least for one ^{13}C-CH_4 data set[59]. Finally, trends in the magnitude of the OH CH_4 sink, which remain uncertain over decadal timescales, can still modulate these incomplete conclusions[34].

The increase resumes from 2006 onwards. Atmospheric CH_4 levels resumed growth after 2006[14], with inferred global emissions being 17–22 Tg CH_4 yr^{-1} greater around 2010 than around 2005 (five-year basis averages; top of Fig. 4). Several studies concluded that a recent surge in natural wetland emissions is one main cause of increasing CH_4 levels, in response to abnormally high temperatures in northern high latitudes in 2007, and increased rainfall over tropical wetlands during 2008–2009 and 2010–2011[13,53,60], two La Niña periods[4]. Furthermore, fossil fuel CH_4 emissions probably increased again after 2005, mostly due to the intensification of shale gas and oil extraction in the United States and coal exploitation by the Chinese and Indian economies[45].

After 2005, the three scenarios use fossil fuel emission changes from the EPA inventory, and the average of EPA and EDGAR4.2 inventories for all other sources barring natural wetlands. Microbial and fossil fuel sources for all scenarios show positive trends after 2005, resulting in an increase of global emissions of 23–33 Tg CH_4 yr^{-1} around 2010 as compared to around 2005 (five-year basis averages). This is a 30% overestimation compared with the mean increase derived from the observations
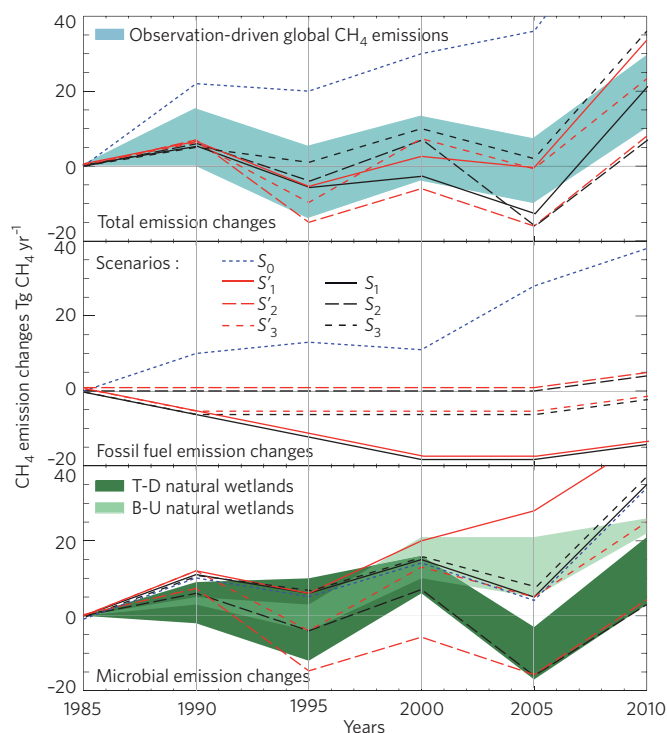

Figure 4 | Plausible scenarios explaining changes in methane emissions over the past three decades. Different lines depict different scenarios of five-year-averaged emission changes since 1985 (see Methods): S_0 (dotted blue lines), S_1 and S'_1 (solid black and red lines), S_2 and S'_2 (long-dashed black and red lines), S_3 and S'_3 (short-dashed black and red lines) Top: range of global CH_4 emission changes (blue shaded area) around a mean inversion (Methods and Supplementary Section ST5). Middle: emission changes from fossil fuels (coal, gas and oil industries). Bottom: emission changes from microbial sources (natural wetlands, rice, animals and waste). The dark and light green shaded areas represent the range of top-down (T-D) and bottom-up (B-U) model results, respectively, for natural wetland emissions.

(17–22 Tg CH_4 yr^{-1}, see above). Thus, either the increase in fossil fuel emissions is overestimated by inventories, or the sensitivity of wetland emissions to precipitation and temperature is too large in some wetland emission models[39]. The contribution of microbial versus fossil emissions to this increase remains largely uncertain; respective contributions vary from 20 to 80%, if accounting for all additional top-down inversions available for the 2000s (Supplementary Fig. S5 and Table 1).

Shortcomings and uncertainty reductions

Our analyses suggest four main shortcomings in the assessment of regional to global CH_4 budgets. First, decadal means and interannual changes in CH_4 emissions from natural wetlands and freshwater systems are too uncertain. It is critically important to improve wetland mapping, both by refining land surface models (for example, through improving estimates of tropical flood plains in hydrological models, specific model developments for peatlands, and the integration of freshwater systems) and by further developing remotely sensed inundation data sets[61] (for instance for dense tropical forests). The scarcity of wetland CH_4 flux measurements and data sets limits the ability to validate large-scale modelled CH_4 emissions for natural wetlands and fresh waters[43]. The extension of the CO_2 FLUXNET measurements and database[62] to CH_4 fluxes is probably achievable at a reasonable cost, and would provide useful constraints for land surface models. For interannual variations in wetland emissions, the sensitivity of emission rates to warming at

high northern latitudes and to rainfall changes in the tropics needs to be more consistently quantified in wetland models. The Amazon drought in 2010[63] should have resulted in a drop in wetland CH_4 emissions, and ongoing analyses may allow researchers to test the hypothesis that tropical wetland CH_4 emissions respond strongly to rainfall anomalies and trends.

Second, the partitioning of CH_4 emissions by region and process is not sufficiently constrained by atmospheric observations in top-down models. Regional partitioning of total emissions would benefit from denser and more evenly distributed CH_4 concentration data. This can be achieved by further developing synergies between high precision monitoring of the surface and the lower atmosphere, including poorly sampled key areas such as the Amazon Basin, Siberia and tropical Africa on one hand, and retrievals of global-scale CH_4 columns by satellites and by high precision remote sensing from the ground on the other. Including continuous measurements of the $\delta^{13}C$ stable isotope ($^{13}CH_4$) at surface stations would help separate biogenic emissions from other sources. Measurements of the δD stable isotope (CH_3D) would provide constraints on the uncertain OH CH_4 sink, which can also be constrained by new proxy tracers[33,34]. Radiocarbon CH_4 data ($^{14}CH_4$) would help constrain the uncertain fossil part of CH_4 emissions, if $^{14}CH_4$ emissions from nuclear installations can be accurately estimated[37]. Estimating long-term trends of fluxes and concentrations requires equally long-term observations, which in turn require stable and coordinated networks[64].

Third, decadal trends in natural and anthropogenic emissions are still very uncertain and limit our ability to definitively attribute changes in emissions from specific sources to observed atmospheric changes since the 1990s. In addition to the (already noted) improvements in land surface models required, inventories for anthropogenic emissions should systematically include an uncertainty assessment, and should improve their representation of emission trends (for instance by more frequently updating the time-dependent factors used in their calculations).

Fourth, uncertainties in the modelling of atmospheric transport and chemistry limit the optimal assimilation of atmospheric observations by increasing uncertainties in top-down inversions. Such uncertainties are also only partly estimated in current inversions. We therefore recommend the continuation of ongoing international model inter-comparisons, which can provide a quantification of transport and chemistry errors to be included in top-down inversions[65,66].

From challenge to opportunity

Our decadal CH_4 budgets reveal that bottom-up models may overestimate total natural CH_4 emissions. The various emission scenarios tested — designed to explain the temporal changes in atmospheric CH_4 levels observed in this and previous studies — suggest that the stabilization of atmospheric CH_4 in the early 2000s is likely to be due to a reduction in or stabilization of fossil fuel emissions, combined with a stabilization of or increase in microbial emissions. After 2006, the renewed global increase in atmospheric CH_4 is consistent with higher emissions from wetlands and fossil fuel burning, but the relative contributions remain uncertain.

In the context of climate change mitigation, atmospheric CH_4 poses both an opportunity and a challenge. The challenge lies in more accurately quantifying the CH_4 budget and its variations. Our synthesis suggests that improvements in models of natural wetland and freshwater emissions, the integration of surface networks monitoring CH_4 concentrations and fluxes (including isotopic composition) and new satellite missions (including active space-borne observations[67]), improvements in anthropogenic emission trends in inventories, and uncertainty reductions in models of atmospheric transport and chemistry, could all help. The opportunity lies in the possibility of developing short-term

climate change mitigation policies that take advantage of the relatively short atmospheric lifetime of CH_4 of about 10 years, and the known technological and agronomical options available for reducing emissions[68].

The potential intensive exploitation of natural gas from shale formations around the world may lead to significant additional CH_4 release into the atmosphere[69], although the potential magnitude of these emissions is still debated[70]. Such additional emissions, and combustion of this 'new' fossil fuel source, may offset mitigation efforts and accelerate climate change. In the longer term, the thawing of permafrost or hydrates could increase CH_4 emissions significantly, and introduce large positive feedbacks to long-term climate change[71]. A better quantification of the global CH_4 budget, with regular updates as done for carbon dioxide[72], will be key to both embracing the opportunities and meeting the challenge.

Methods

Data analysis. Top-down and bottom-up studies addressing the evolution of the CH_4 cycle after 1980 and covering at least five years of a decade were gathered. Therefore, the number and the nature of studies used in this work vary from one decade to another. Top-down inversions include atmospheric chemistry transport models and assimilation systems[19,46,53,73–77]. Bottom-up approaches comprise modelling studies for wetland[40–42] and biomass-burning emissions[47,78–80], emission inventories for anthropogenic[55,56,81] and natural sources[82], and a suite of atmospheric chemistry models within the ACCMIP intercomparison project providing CH_4 chemical loss[30,39,83].

The monthly fluxes (emissions and sinks) provided by the different groups were post-processed similarly. They were re-gridded on a common grid ($1° \times 1$) and converted into the same units (Tg CH_4 per grid cell); then monthly, annual and decadal means were computed for 12 regions based on the TransCom[84] intercomparison map, with subdivisions in high-emission regions. Regional and global means were used to construct Figs 1, 2 and 3, Supplementary Figs S2 and S3, Table 1 and Supplementary Tables S2 and S3.

The reported ranges and error bars represent the minimum and maximum values obtained among the different studies (Figs 1, 3 and 4 and Table 1). The small number of studies for some categories makes it difficult to properly apply a standard deviation.

Interannual variability (IAV) was computed as the difference between the 12-month running mean and the long-term mean. However a consistent period for estimating the long-term mean was not compatible with all data sources (Supplementary Fig. S5).

Observation-driven global CH_4 emissions. For 'attribution of temporal changes', we used the only top-down study that estimates CH_4 emissions over the past 30 years[53] with five different set-ups. The mean of these five inversions was assumed to represent average global emissions. However these five inversions only partially represented the full range of global CH_4 emissions, due to differences in prior emission scenarios and errors, observations and their errors, OH fields and atmospheric transport representation. To estimate the full range of global CH_4 emissions we complemented the mean inversion with a sensitivity analysis based on a one-box model for the whole atmosphere[54]. The change in the global burden of CH_4 is given by:

$$\frac{d[CH_4]}{dt} = E - \frac{[CH_4]}{\tau} \qquad (1)$$

where $[CH_4]$ is the global CH_4 burden, E is the sum of all emissions, and τ is the total atmospheric CH_4 lifetime. Equation (1) can be rearranged to calculate the annual CH_4 source strength E as follows:

$$E = \frac{d[CH_4]}{dt} + \frac{[CH_4]}{\tau} \qquad (2)$$

In this equation, the annual increase $d[CH_4]/dt$ and the burden $[CH_4]$ were given by the yearly–averaged growth rates and mole fractions of Fig. 1. Global CH_4 emissions were generated by computing emissions with equation (2) for each of the four networks and for a lifetime τ varying from 8 to 10 years to include uncertainties in OH changes[34,85]. Minimum and maximum values of E were extracted for five-year periods to produce the range of emissions plotted around the mean of atmospheric inversions (blue shaded area in Fig. 4, top panel).

Emission scenarios. The emission scenarios are based on five-year average CH_4 fluxes around the years 1985, 1990, 1995, 2000, and 2005. For 2010 we used available years between 2008 and 2012, mainly before 2010. Flux changes from 2005 to 2010 might be slightly biased by missing years after 2010. For example, fossil and microbial emissions both increase between 2005 and 2009; if after 2010 these emissions were further increasing (or decreasing), then the 2005-2010 changes will be underestimated (or overestimated). We assume that such a potential bias does not modify the (mostly) qualitative message of our scenario analysis. The five-year

changes from biomass burning remain small (<2 Tg CH_4 per five-year period) and were not considered here.

The scenarios presented in Fig. 4 use either natural wetland emissions from top-down inversions (S_x) or bottom-up models (S'_x). Other data are taken from recent publications and EDGAR4.2 and EPA inventories.

S_0 and S'_0 are built by summing the mean wetland emissions from inversions and the mean of EPA (ref. 55) and EDGAR4.2 (ref. 56) 'other' emissions. Scenarios S_1 and S'_1 sum the mean wetland emissions with decreasing (1985–2000), constant (2000–2005), and increasing (2005–2010) fossil fuel emissions to be compatible with a recent analysis[15]. Scenarios S_2 and S'_2 sum the mean wetland emissions with constant (1985–2005) and increasing (2005–2010) fossil fuel emissions. Other microbial emissions (mean of EPA and EDGAR) are scaled to a recent study[58]. Scenarios S_3 and S'_3 sum the mean wetland emissions with decreasing (1985–1990), constant (1990–2005), and increasing (2005–2010) fossil fuel emissions. Other microbial emissions (mean of EPA and EDGAR) are scaled to remain constant during 1990–2005 according to another recent study[59]. After 2005, all scenarios include fossil fuel emission changes from the EPA inventory, wetland emission changes from inversions or bottom-up studies and other emission changes from the mean of EPA and EDGAR4.2.

References

1. Etheridge, D. M., Pearman, G. I. & Fraser, P. J. Changes in tropospheric methane between 1841 and 1978 from a high accumulation-rate Antarctic ice core. *Tellus* **44B**, 282–294 (1992).
2. Blake, D. R. *et al.* Global increase in atmospheric methane concentrations between 1978 and 1980. *Geophys. Res. Lett.* **9**, 477–480 (1982).
3. Cunnold, D. M. *et al. In situ* measurements of atmospheric methane at GAGE/AGAGE sites during 1985–2000 and resulting source inferences. *J. Geophys. Res.: Atmos.* http://dx.doi.org/10.1029/2001jd001226 (2002).
4. Dlugokencky, E. J. *et al.* Observational constraints on recent increases in the atmospheric CH burden. *Geophys. Res. Lett.*, **36**, L18803 (2009).
5. Francey, R. J., Steele, L. P., Langenfelds, R. L. & Pak, B. C. High precision long-term monitoring of radiatively active and related trace gases at surface sites and from aircraft in the southern hemisphere atmosphere. *J. Atmos. Sci.* **56**, 279–285 (1999).
6. World Data Centre for Greenhouse Gases (WMO/WDCGG) (2012); http://ds.data.jma.go.jp/gmd/wdcgg/introduction.html.
7. Brenninkmeijer, C. A. M. *et al.* Civil Aircraft for the regular investigation of the atmosphere based on an instrumented container: The new CARIBIC system. *Atmos. Chem. Phys.* **7**, 4953–4976 (2007).
8. Wecht, K. J. *et al.* Validation of TES methane with HIPPO aircraft observations: implications for inverse modeling of methane sources. *Atmos. Chem. Phys.* **12**, 1823–1832 (2012).
9. Schuck, T. J. *et al.* Distribution of methane in the tropical upper troposphere measured by CARIBIC and CONTRAIL aircraft. *J. Geophys. Res.: Atmos.* **117**, D19304 (2012).
10. Crevoisier, C. *et al.* Tropospheric methane in the tropics — first year from IASI hyperspectral infrared observations. *Atmos. Chem. Phys.* **9**, 6337–6350 (2009).
11. Frankenberg, C. *et al.* Global column-averaged methane mixing ratios from 2003 to 2009 as derived from SCIAMACHY: Trends and variability. *J. Geophys. Res.: Atmos.* **116**, D04302 (2011).
12. Morino, I. *et al.* Preliminary validation of column-averaged volume mixing ratios of carbon dioxide and methane retrieved from GOSAT short-wavelength infrared spectra. *Atmos. Meas. Tech.* **4**, 1061–1076 (2011).
13. Dlugokencky, E. J., Nisbet, E. G., Fisher, R. & Lowry, D. Global atmospheric methane: budget, changes and dangers. *Phil. Trans. R. Soc. A* **369**, 2058–2072 (2011).
14. Rigby, M. *et al.* Renewed growth of atmospheric methane. *Geophys. Res. Lett.* **35**, L22805 (2008).
15. Simpson, I. J. *et al.* Long-term decline of global atmospheric ethane concentrations and implications for methane. *Nature* **488**, 490–494 (2012).
16. Denman, K. L. *et al.* in *IPCC Climate Change 2007: Couplings Between Changes in the Climate System and Biogeochemistry* (eds Solomon, S. *et al.*) (Cambridge Univ. Press; 2007).
17. Cicerone, R. J. & Oremland, R. S. Biogeochemical aspects of atmospheric methane. *Glob. Biogeochem. Cycles* **2**, 299–327 (1988).
18. Ehhalt, D. H. The atmospheric cycle of methane. *Tellus* **26**, 58–70 (1974).
19. Fung, I. *et al.* Three-dimensional model synthesis of global methane cycle. *J. Geophys. Res.* **96**, 13033–13065 (1991).
20. Monteil, G. *et al.* Interpreting methane variations in the past two decades using measurements of CH_4 mixing ratio and isotopic composition. *Atmos. Chem. Phys.* **11**, 9141–9153 (2011).
21. Bousquet, P. *et al.* Contribution of anthropogenic and natural sources to atmospheric methane variability. *Nature* **443**, 439–443 (2006).
22. Neef, L., van Weele, M. & van Velthoven, P. Optimal estimation of the present-day global methane budget. *Glob. Biogeochem. Cycles* **24**, GB4024 (2010).
23. Wahlen, M., Tanaka, N., Henry, R. & Yoshinari, T. ^{13}C, D and ^{14}C in methane. *Eos* **68**, 1220 (1987).
24. Fisher, R. E. *et al.* Arctic methane sources: Isotopic evidence for atmospheric inputs. *Geophys. Res. Lett.* **38**, L21803 (2011).
25. Keppler, F., Hamilton, J. T. G., Brass, M. & Rockmann, T. Methane emissions from terrestrial plants under aerobic conditions. *Nature* **439**, 187–191 (2006).
26. Nisbet, R. E. R. *et al.* Emission of methane from plants. *Proc. R. Soc. B-Biol. Sci.* **276**, 1347–1354 (2009).
27. Curry, C. L. Modeling the soil consumption of atmospheric methane at the global scale. *Glob. Biogeochem. Cycles* **21**, GB4012 (2007).
28. Zhuang, Q. *et al.* Methane fluxes between terrestrial ecosystems and the atmosphere at northern high latitudes during the past century: A retrospective analysis with a process-based biogeochemistry model. *Glob. Biogeochem. Cycles* **18**, GB3010 (2004).
29. Allan, W., Struthers, H. & Lowe, D. C. Methane carbon isotope effects caused by atomic chlorine in the marine boundary layer: Global model results compared with Southern Hemisphere measurements. *J. Geophys. Res.: Atmos.* **112**, D04306 (2007).
30. Naik, V. *et al.* Preindustrial to present day changes in tropospheric hydroxyl radical and methane lifetime from the Atmospheric Chemistry and Climate Model Intercomparison Project (ACCMIP). *Atmos. Chem. Phys.* **13**, 5277–5298 (2013).
31. Bastviken, D., Tranvik, L. J., Downing, J. A., Crill, P. M. & Enrich-Prast, A. Freshwater methane emissions offset the continental carbon sink. *Science* **331**, 50 (2011).
32. Walter, K. M., Smith, L. C. & Stuart Chapin, F. Methane bubbling from northern lakes: present and future contributions to the global methane budget. *Phil. Trans. R. Soc. A* **365**, 1657–1676 (2007).
33. Huang, J. & Prinn, R. G. Critical evaluation of emissions of potential new gases for OH estimation. *J. Geophys. Res.* **107**, 4784 (2002).
34. Montzka, S. A. *et al.* Small interannual variability of global atmospheric hydroxyl. *Science* **331**, 67–69 (2011).
35. Etiope, G., Lassey, K. R., Klusman, R. W. & Boschi, E. Reappraisal of the fossil methane budget and related emission from geologic sources. *Geophys. Res. Lett.* **35**, L09307 (2008).
36. Shakhova, N. *et al.* Extensive methane venting to the atmosphere from sediments of the East Siberian Arctic Shelf. *Science* **327**, 1246 (2010).
37. Lassey, K. R., Lowe, D. C. & Smith, A. M. The atmospheric cycling of radiomethane and the "fossil fraction" of the methane source. *Atmos. Chem. Phys.* **7**, 2141–2149 (2007).
38. Voulgarakis, A. *et al.* Analysis of present day and future OH and methane lifetime in the ACCMIP simulations. *Atmos. Chem. Phys.* **13**, 2563–2587 (2013).
39. Melton, J. R. *et al.* Present state of global wetland extent and wetland methane modelling: conclusions from a model intercomparison project (WETCHIMP). *Biogeosciences* **10**, 753–788 (2013).
40. Hodson, E. L., Poulter, B., Zimmermann, N. E., Prigent, C. & Kaplan, J. O. The El Niño Southern Oscillation and wetland methane interannual variability. *Geophys. Res. Lett.* **38**, L08810 (2011).
41. Ringeval, B. *et al.* Climate-CH_4 feedback from wetlands and its interaction with the climate-CO_2 feedback. *Biogeosciences* **8**, 2137–2157 (2011).
42. Spahni, R. *et al.* Constraining global methane emissions and uptake by ecosystems. *Biogeosciences* **8**, 1643–1665 (2011).
43. Riley, W. J. *et al.* Barriers to predicting changes in global terrestrial methane fluxes: analyses using CLM4Me, a methane biogeochemistry model integrated in CESM. *Biogeosciences* **8**, 1925–1953 (2011).
44. Mastrandrea, M. D. *et al. Guidance Note for Lead Authors of the IPCC Fifth Assessment Report on Consistent Treatment of Uncertainties* (IPCC, 2010); http://www.ipcc.ch.
45. Ohara, T. *et al.* An Asian emission inventory of anthropogenic emission sources for the period 1980–2020 *Atmos Chem Phys* **7**, 4419–4444 (2007).
46. Bergamaschi, P. *et al.* Inverse modeling of global and regional CH4 emissions using SCIAMACHY satellite retrievals. *J. Geophys. Res.* http://dx.doi.org/10.1029/2009JD012287 (2009).
47. Van der Werf, G. R. *et al.* Global fire emissions and the contribution of deforestation, savanna, forest, agricultural, and peat fires (1997–2009). *Atmos. Chem. Phys.* **10**, 11707–11735 (2010).
48. Sanderson, M. G. Biomass of termites and their emissions of methane and carbon dioxide: A global database. *Glob. Biogeochem. Cycles* **10**, 543–557 (1996).
49. Bousquet, P., Hauglustaine, D. A., Peylin, P., Carouge, C. & Ciais, P. Two decades of OH variability as inferred by an inversion of atmospheric transport and chemistry of methyl chloroform. *Atmos. Chem. Phys.* **5**, 2635–2656 (2005).

50. Simpson, I. J., Rowland, F. S., Meinardi, S. & Blake, D. R. Influence of biomass burning during recent fluctuations in the slow growth of global tropospheric methane. *Geophys. Res. Lett.* **33,** L22808 (2006).

51. Dlugokencky, E. J. *et al.* Changes in CH_4 and CO growth rates after the eruption of Mt Pinatubo and their link with changes in tropical tropospheric UV flux. *Geophys. Res. Lett.* **23,** 2761–2764 (1996).

52. Langenfelds, R. L. *et al.* Interannual growth rate variations of atmospheric CO_2 and its delta ^{13}C, H_2, CH_4, and CO between 1992 and 1999 linked to biomass burning. *Glob. Biogeochem. Cycles* **16,** 1048 (2002).

53. Bousquet, P. *et al.* Source attribution of the changes in atmospheric methane for 2006–2008 *Atmos. Chem. Phys.* **11,** 3689–3700 (2011).

54. Dlugokencky, E. J., Masarie, K. A., Lang, P. M. & Tans, P. P. Continuing decline in the growth rate of the atmospheric methane burden. *Nature* **393,** 447–450 (1998).

55. Environmental Protection Agency. Global Anthropogenic Non-CO_2 Greenhouse Gas Emissions: 1990–2030. (US Environmental Protection Agency, 2011).

56. European Commission, Joint Research Centre/Netherlands Environmental Assessment Agency. Emission Database for Global Atmospheric Research (EDGAR) (version 4.2) (2011); http://edgar.jrc.ec.europa.eu.

57. Aydin, M. *et al.* Recent decreases in fossil-fuel emissions of ethane and methane derived from firn air. *Nature* **476,** 198–201 (2011).

58. Kai, F. M., Tyler, S. C., Randerson, J. T. & Blake, D. R. Reduced methane growth rate explained by decreased Northern Hemisphere microbial sources. *Nature* **476,** 194–197 (2011).

59. Levin, I. *et al.* No inter-hemispheric $\delta^{13}CH_4$ trend observed. *Nature* **486,** E3–E4 (2012).

60. Bloom, A. A., Palmer, P. I., Fraser, A., Reay, D. S. & Frankenberg, C. Large-scale controls of methanogenesis inferred from methane and gravity spaceborne data. *Science* **327,** 322–325 (2010).

61. Prigent, C., Papa, F., Aires, F., Rossow, W. B. & Matthews, E. Global inundation dynamics inferred from multiple satellite observations, 1993–2000. *J. Geophys. Res.* **112,** D12107 (2007).

62. FLUXNET database; http://fluxnet.ornl.gov.

63. Lewis, S. L., Brando, P. M., Phillips, O. L., van der Heijden, G. M. F. & Nepstad, D. The 2010 Amazon drought. *Science* **331,** 554–554 (2011).

64. Houweling, S. *et al.* Iconic CO2 Time Series at Risk. *Science* **337,** 1038–1040 (2012).

65. Lamarque, J. F. *et al.* The Atmospheric Chemistry and Climate Model Intercomparison Project (ACCMIP): overview and description of models, simulations and climate diagnostics. *Geosci. Model Dev.* **6,** 179–206 (2013).

66. Patra, P. K. *et al.* TransCom model simulations of CH_4 and related species: linking transport, surface flux and chemical loss with CH_4 variability in the troposphere and lower stratosphere. *Atmos. Chem. Phys.* **11,** 12813–12837 (2011).

67. Kiemle, C. *et al.* Sensitivity studies for a space-based methane lidar mission. *Atmos. Meas. Tech.* **4,** 2195–2211 (2011).

68. Shindell, D. *et al.* Simultaneously mitigating near-term climate change and improving human health and food security. *Science* **335,** 183–189 (2012).

69. Howarth, R., Santoro, R. & Ingraffea, A. Methane and the greenhouse-gas footprint of natural gas from shale formations. *Climatic Change* **106,** 679–690 (2011).

70. Cathles, L., Brown, L., Taam, M. & Hunter, A. A commentary on "The greenhouse-gas footprint of natural gas in shale formations" by R. W. Howarth, R. Santoro, and Anthony Ingraffea. *Climatic Change* **113,** 525–535 (2012).

71. Koven, C. D. *et al.* Permafrost carbon-climate feedbacks accelerate global warming. *Proc. Natl Acad. Sci. USA* **108,** 14769–14774 (2011).

72. Global Carbon Project (2013); http://www.globalcarbonproject.org/index.htm.

73. Bruhwiler, L., Dlugokencky, E. J. & Masarie, K. *AGU Fall Meeting* abstr. B11G-01 (2011).

74. Chen, Y. H. & Prinn, R. G. Estimation of atmospheric methane emissions between 1996 and 2001 using a three-dimensional global chemical transport model. *J. Geophys. Res.* **111,** D10307 (2006).

75. Fraser, A. *et al.* Estimating regional methane surface fluxes: the relative importance of surface and GOSAT mole fraction measurements. *Atmos. Chem. Phys.* **13,** 5697–5713 (2013).

76. Hein, R., Crutzen, P. J. & Heimann, M. An inverse modeling approach to investigate the global atmospheric methane cycle. *Glob. Biogeochem. Cycles* **11,** 43–76 (1997).

77. Pison, I., Bousquet, P., Chevallier, F., Szopa, S. & Hauglustaine, D. Multi-species inversion of CH4, CO and H-2 emissions from surface measurements. *Atmos. Chem. Phys.* **9,** 5281–5297 (2009).

78. Mieville, A. *et al.* Emissions of gases and particles from biomass burning during the 20th century using satellite data and an historical reconstruction. *Atmos. Environ.* **44,** 1469–1477 (2010).

79. Van het Bolscher, M. *et al.* Emission data sets and methodologies for estimating emissions (eds Schultz, M. G. & Rast, S.) (2007).

80. Wiedinmyer, C. *et al.* The Fire INventory from NCAR (FINN): a high resolution global model to estimate the emissions from open burning. *Geosci. Model Dev.* **4,** 625–641 (2011).

81. Dentener, F. *et al.* The impact of air pollutant and methane emission controls on tropospheric ozone and radiative forcing: CTM calculations for the period 1990–2030 *Atmos. Chem. Phys.* **5,** 1731–1755 (2005).

82. Environmental Protection Agency. Methane and Nitrous Oxide Emissions From Natural Sources. (US Environmental Protection Agency, 2010).

83. Williams, J. E., Strunk, A., Huijnen, V. & van Weele, M. The application of the Modified Band Approach for the calculation of on-line photodissociation rate constants in TM5: implications for oxidative capacity. *Geosci. Model Dev.* **5,** 15–35 (2012).

84. Gurney, K. R. *et al.* Transcom 3 inversion intercomparison: Model mean results for the estimation of seasonal carbon sources and sinks. *Glob. Biogeochem. Cycles* **18,** GB2010 (2004).

85. Prinn, R. G. *et al.* Evidence for substantial variations of atmospheric hydroxyl radicals in the past two decades. *Science* **292,** 1882–1888 (2001).

86. Beck, V. *et al.* Methane airborne measurements and comparison to global models during BARCA. *Journal of Geophysical Research: Atmospheres* **117,** D15310 (2012).

87. Dickens, G. R. Methane hydrates in quaternary climate change — The clathrate gun hypothesis. *Science* **299,** 1017–1017 (2003).

88. Hoelzemann, J. J., Schultz, M. G., Brasseur, G. P., Granier, C. & Simon, M. Global Wildland Fire Emission Model (GWEM): Evaluating the use of global area burnt satellite data. *J. Geophys. Res.* **109,** D14S04 (2004).

89. Ito, A. & Penner, J. E. Global estimates of biomass burning emissions based on satellite imagery for the year 2000. *J. Geophys. Res.* **109,** D14S05 (2004).

90. Rhee, T. S., Kettle, A. J. & Andreae, M. O. Methane and nitrous oxide emissions from the ocean: A reassessment using basin-wise observations in the Atlantic. *J. Geophys. Res.* **114,** D12304 (2009).

91. Sugimoto, A., Inoue, T., Kirtibutr, N. & Abe, T. Methane oxidation by termite mounds estimated by the carbon isotopic composition of methane. *Glob. Biogeochem. Cycles* **12,** 595–605 (1998).

92. Kasibhatla, K. *et al. Inverse Methods in Global Biogeochemical Cycles, Volume 114* (AGU, 2000).

93. Rodgers, C. D. *Inverse Methods for Atmospheric Sounding: Theory and Practice* (World Scientific, 2000).

94. Krol, M. & Lelieveld, J. Can the variability in tropospheric OH be deduced from measurements of 1,1,1-trichloroethane (methyl chloroform)? *J. Geophys. Res.* **108,** 4125 (2003).

Author contributions

S.K., P. Bousquet, P.C., J.G.C. and C.L.Q. designed the study and provided conceptual advice. S.K., P. Bousquet and M. Saunois processed data sets, developed figures and wrote the manuscript. E.J.D., M. Schmidt, P.J.F., P.B.K., L.P.S., R.L.L., R.G.P., M.R., R.F.W., D.R.B. and I.J.S. provided atmospheric *in situ* data. P.Bousquet, P.Bergamaschi, L.B., F.C., L.F., A.F., S.H., P.I.P. and I.P. provided top-down inversion results (all five emission categories). S.C., E.L.H., B.P., B.R., M.Santini, R.S. and G.R.v.d.W provided bottom-up modelling and inventory data sets for wetland, biomass burning and termite emissions. D.B., P.C.-S., B.J., J.-F.L., V.N., D.P., D.T.S., S.A.S., K.S., S.S., A.V., M.v.W., J.E.W. and G.Z. provided bottom-up estimates of CH_4 loss due to OH. All authors contributed extensively to the work presented in this paper, and to revisions of the manuscript.

Additional information

Reprints and permissions information is available online at www.nature.com/reprints. Correspondence should be addressed to philippe.bousquet@lsce.ipsl.fr.

Competing financial interests

The authors declare no competing financial interests.

Stefanie Kirschke[1], Philippe Bousquet[1]*, Philippe Ciais[1], Marielle Saunois[1], Josep G. Canadell[2], Edward J. Dlugokencky[3], Peter Bergamaschi[4], Daniel Bergmann[5], Donald R. Blake[6], Lori Bruhwiler[3], Philip Cameron-Smith[5], Simona Castaldi[7,8], Frédéric Chevallier[1], Liang Feng[9], Annemarie Fraser[9], Martin Heimann[10], Elke L. Hodson[11], Sander Houweling[12,13], Béatrice Josse[14], Paul J. Fraser[15], Paul B. Krummel[15], Jean-François Lamarque[16], Ray L. Langenfelds[15], Corinne Le Quéré[17], Vaishali Naik[18], Simon O'Doherty[19], Paul I. Palmer[9], Isabelle Pison[1], David Plummer[20], Benjamin Poulter[1], Ronald G. Prinn[21], Matt Rigby[22], Bruno Ringeval[13,23,24], Monia Santini[8], Martina Schmidt[1], Drew T. Shindell[25], Isobel J. Simpson[6], Renato Spahni[26], L. Paul Steele[15], Sarah A. Strode[27,28], Kengo Sudo[29], Sophie Szopa[1], Guido R. van der Werf[30], Apostolos Voulgarakis[25,31], Michiel van Weele[32], Ray F. Weiss[33], Jason E. Williams[32] and Guang Zeng[34]

[1]LSCE-CEA-UVSQ-CNRS, Orme des Merisiers, 91190 Gif-sur-Yvette, France, [2]Global Carbon Project, CSIRO Marine and Atmospheric Research, GPO Box 3023, Canberra, ACT 2601, Australia, [3]NOAA ESRL, 325 Broadway, Boulder, Colorado 80305, USA, [4]Institute for Environment and Sustainability, Joint Research Centre, TP290, I-21027 Ispra (Va), Italy, [5]Lawrence Livermore National Laboratory, PO Box 808, Livermore, California 94551-0808, USA, [6]University of California Irvine, 570 Rowland Hall, Irvine, California 92697, USA, [7]Department of Environmental Sciences, Second University of Naples, via Vivaldi 43, 81100 Caserta, Italy, [8]Centro Euro-Mediterraneo sui Cambiamenti Climatici (CMCC), via Augusto Imperatore 16, 73100 Lecce, Italy, [9]School of Geosciences, University of Edinburgh, Crew Building, West Mains Road, Edinburgh, EH9 3JN, UK, [10]Max Planck Institute for Biogeochemistry, PF 100164, D-07701 Jena, Germany, [11]Swiss Federal Research Institute WSL, Zuercherstrasse 111, 8903 Mensdorf, Switzerland, [12]SRON, Netherlands Institute for Space Research, Sorbonnelaan 2, 3584 CA Utrecht, The Netherlands, [13]Institue for Marine and Atmospheric Research Utrecht, Sorbonnelaan 2, 3584 CA Utrecht, The Netherlands, [14]Météo France, CNRM/GMGEC/CARMA, 42 av G. Coriolis, 31057 Toulouse, France, [15]Centre for Australian Weather and Climate Research/CSIRO Marine and Atmospheric Research, Aspendale, Victoria 3195, Australia, [16]NCAR, PO Box 3000, Boulder, Colorado 80307-3000, USA, [17]Tyndall Centre for Climate Change Research, University of East Anglia, Norwich Research Park, Norwich, NR4 7TJ, UK, [18]UCAR/NOAA Geophysical Fluid Dynamics Laboratory, 201 Forrestal Road, Princeton, New Jersey 08540, USA, [19]University of Bristol, Office Old Park Hill, Cantock's Close, Clifton, Bristol BS8 1TS, UK, [20]Canadian Centre for Climate Modelling and Analysis, Environment Canada, 550 Sherbrooke Street West, West Tower, Montréal, Quebec, H3A 1B9, Canada, [21]Massachusetts Institute of Technology, Building 54-1312, Cambridge, Massachusetts 02139-2307, USA, [22]School of Chemistry, University of Bristol, Cantocks Close, Bristol BS8 1TS, UK, [23]IMAU, Utrecht University, Princetonplein 5, 3584 CC Utrecht, The Netherlands, [24]Department of Systems Ecology, VU University Amsterdam, De Boelelaan 1085, 1081 HV Amsterdam, The Netherlands, [25]NASA Goddard Institute for Space Studies, 2880 Broadway, New York, New York 10025, USA, [26]University of Bern, Physics Institute, Climate and Environmental Physics, Sidlerstrasse 5, CH-3012 Bern, Switzerland, [27]NASA Goddard Space Flight Centre, Greenbelt, Maryland 20771, USA, [28]Universities Space Research Association, NASA Goddard Space Flight Centre, Greenbelt, Maryland 20771, USA, [29]Graduate School of Environmental Studies, Nagoya University Furo-cho, Chikusa-ku, Nagoya 464-8601, Japan, [30]VU University, Faculty of Earth and Life Sciences, De Boelelaan 1085, 1081 HV Amsterdam, The Netherlands, [31]Department of Physics, Imperial College London, London SW7 2AZ, UK, [32]Royal Netherlands Meteorological Institute (KNMI), PO Box 201, 3730 AE De Bilt, The Netherlands, [33]Scripps Institution of Oceanography, UCSD, La Jolla, California 92093-0244, USA, [34]National Institute of Water and Atmospheric Research, Private Bag 50061, Omakau, Central Otago 9352, New Zealand. *e-mail: Philippe.Bousquet@lsce.ipsl.fr